ChemComm

Accepted Manuscript

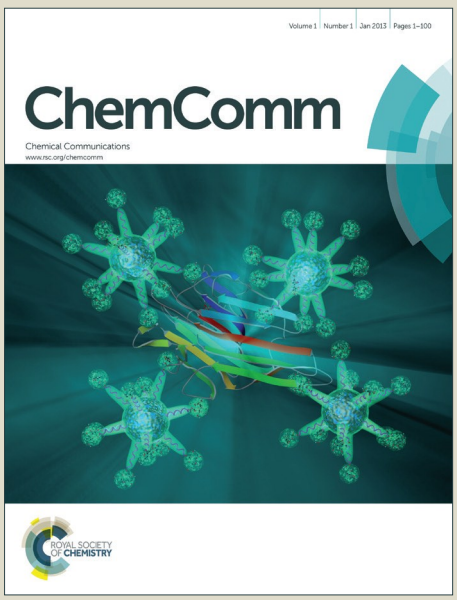

ROYAL SOCIETY OF CHEMISTRY

www.rsc.org/chemcomm

Journal Name

RSCPublishing

COMMUNICATION

Ellipsoid-Shaped Superparamagnetic Nanoclusters through Emulsion Electrospinning

Cite this: DOI: 10.1039/x0xx00000x

Markus B. Bannwarth[a*], Agathe Camerlo[a], Sebastian Ulrich[a], Gerhard Jakob[b], Giuseppino Fortunato[a], René M. Rossi[a], Luciano F. Boesel[a*]

Received 00th January 2012,
Accepted 00th January 2012

DOI: 10.1039/x0xx00000x

www.rsc.org/

Ellipsoid-shaped nanoclusters composed of single superparamagnetic nanoparticles can be generated by emulsion electrospinning. Stretching and subsequent solvent evaporation of iron oxide loaded emulsion droplets during the emulsion electrospinning process enables the creation of such structures embedded in polymer nanofibers. Dissolution of the polymer fibers yields an aqueous dispersion of the inorganic clusters which are the first example of ellipsoid-shaped superparamagnetic nanoclusters with a high saturation magnetization (~47 emu·g^{-1}).

Superparamagnetic nanoparticles have drawn tremendous attention in the field of biomedical applications.[1] Thanks to their strong response to external magnetic fields, they are powerful contrast enhancers for magnetic resonance imaging (MRI)[2, 3] and heat sources for hyperthermia[4] or triggered drug release.[5] The superparamagnetic effect is strongly size-limited and only exists for iron oxide nanoparticles that are smaller than about 20 nm.[6] However, superparamagnetic particles can be clustered to preserve and even improve their properties.[7, 8] Implementing them as contrast agents for MRI, their nature to shorten the transverse relaxation of water is enhanced, since they collectively act as nanoparticle ensemble.[9] Today, many examples for spherical superparamagnetic nanoparticle clusters are explained in literature.[10] However their ellipsoid analogues are found very rarely, even if shape anisotropy is considered to impose a very strong influence on the magnetization properties.[11] Anisotropic magnetic materials are believed to possess great potential in magnetomechanical systems, high density data storage systems or sensing applications.[12] Additionally, shape plays a major role for nanoparticle-cell interactions[13, 14] or for nanoparticle drying/patterning on surfaces.[15] Besides assembling superparamagnetic nanoclusters into linear chains to create one-dimensionality (1D),[16-18] Nanoparticles with ellipsoid shape are accessible as hematites and goethites.[19-21] However, the described iron oxide based rices/ellipsoids either reach a rather low saturation magnetization of ~ 10 emu·g^{-1} or lower (and between 2-26 emu·g^{-1} for different Mn-, Ni-, Cu-, Sn-doped samples) and/or show a significant remanence. Since superparamagnetic iron oxides can reach values of >90 emu·g^{-1},[22] the saturation magnetization of ellipsoid-shape superparamagnetic nanoparticle clusters can still be strongly improved and novel methods for their preparation are required.[23]

Hence, the question arises whether there is a possibility to cluster single superparamagnetic nanocrystals permanently in an ellipsoid shape. Indeed, this becomes possible when making use of an elongation-evaporation process that can be applied *via* electrospinning to an aqueous emulsion containing octane droplets with a high loading of superparamagnetic nanoparticles (Figure 1). The process is inspired by the elongation of solvent-swollen polymer nanoparticles during the electrospinning process.[24] For axial deformation of initially spherical to elongated droplets, it is mandatory to apply a unidirectional stress on the droplet. It is well known that during the electrospinning process stresses of 10-100 kPa are present.[25] Although it is reported that during emulsion electrospinning the droplets can become deformed in the jet whipping area where rapid jet thinning and thus, stress generation occurs,[26] this stretching phenomenon has never been used to make elongated inorganic materials. The possibility to generate ellipsoid-shaped superparamagnetic iron oxide nanoclusters (ESIONCs) *via* emulsion electrospinning is depicted in Figure 1. Firstly, easily accessible oleate-capped iron oxide nanoparticles with superparamagnetic properties were redispersed in high solid contents (50 wt.%) in *n*-octane. Octane is very suitable for the redispersion of the oleate-capped iron oxide nanoparticles.[27] By addition of this dispersion to a continuous aqueous phase containing sodium dodecylsulfate (SDS) as surfactant and application of ultrasonic treatment, a miniemulsion of octane nanodroplets with a high content of iron oxide nanoparticles is formed. This miniemulsion is mixed with an aqueous poly (vinyl alcohol) (PVA) solution to yield in a miniemulsion containing 10 wt.% of PVA. The viscous

miniemulsion is then inserted in the electrospinning process. During electrospinning, the elongation-evaporation process occurs. Here, the continuous PVA/water phase is spun to form nanofibers while the disperse phase of superparamagnetic octane droplets is embedded in the PVA fibers. For the generation of the ESIONCs, thinning of the jet and subsequent evaporation of water leads to a squeezing of the magnetic droplets in direction of the fiber axis. Then, the octane, with its higher boiling point than water (~125 °C), evaporates, and solid ESIONCs are formed from the elongated liquid droplets. When we replaced the octane and used chloroform instead under similar conditions, we could not observe elongated clusters of iron oxide nanoparticles. Instead, spherical clusters were found. Hence, the solvent cannot easily be exchanged.

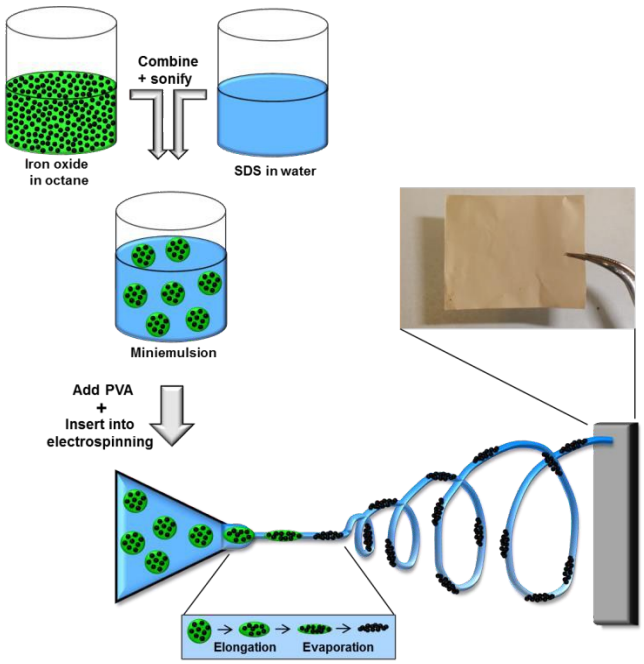

Fig. 1 Schematic illustration of the fabrication of ESIONCs. An octane phase containing iron oxide nanoparticles is mixed with a SDS-containing aqueous solution and sonified to form a direct miniemulsion. After addition of PVA to the miniemulsion, electrospinning is performed. During the electrospinning process, the ESIONCs are formed by elongation and evaporation of the octane droplets. Finally, the ESIONCs are found embedded in the fibrous PVA mesh. Top right: Optical micrograph of a brown-colored electrospun iron oxide/PVA mesh on an aluminum foil.

Investigation of the morphology of the formed fibers and the structure of the incorporated ESIONCs was done with electron microscopy (Figure 2). SEM and STEM overview images show a mesh of nanofibers (Figure 2a+b). A closer look at the interior structure of the fibers reveals an elongated cluster consisting of many single nanoparticles as it is embedded in the fibrous PVA network (Figure 2c).

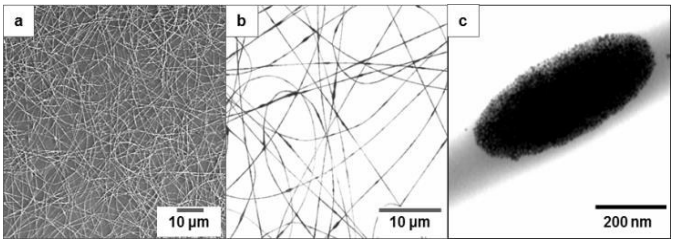

Fig. 2 SEM (a) and STEM (b, c) micrographs of electrospun PVA fibers with incorporated ESIONCs.

Importantly, the elongation of the iron oxide clusters is related to the final fiber diameter. From STEM images, one can clearly see that with a decreasing diameter of the PVA fiber, the elongation of the clusters increases considerably (Figure 3a-f). The elongation, however, is not strongly influenced by the size of the nanoparticle cluster (Average cluster diameter: Equatorial axis: 94±40 nm; Polar axis: 250±114 nm). Similar aspect ratios are obtained for differently sized clusters, whenever the fiber has the same diameter. This phenomenon can be observed especially in the Figures 3d+e, where differently sized clusters are embedded in the same fiber and show similar stretching behavior.

In order to quantify the relationship between the cluster elongation and the fiber diameter, several fibers with different diameters were analyzed and the aspect ratio of the ESIONCs is plotted against the fiber diameter (Figure 3g). The ESIONCs were analyzed from a mesh of nanofibers with various fiber diameters (161±58 nm). Hence, the aspect ratio of the ESIONCs can directly be correlated to the fiber diameter (for a given PVA concentration of 10 wt.%). For fiber diameters above 200 nm, the clusters are only weakly elongated and the aspect ratio lies near 1. When the fiber diameter is lower than 200 nm, efficient stretching is achieved. For the extreme case when the fiber diameter is close to 50 nm, the aspect ratio can be very high, reaching a value of nearly 10. In principle, the fiber diameter is influenced by many electrospinning conditions.[28-30] In order to evaluate the effect on the fiber diameter and the stretching of the clusters, we investigated some of these parameters. When varying the applied voltage (6-12 V) and the distance between tip and collector (15-25 cm), we observed no significant change in the fiber diameter and the aspect ratio of the ESIONCs. In contrast, a variation of the PVA concentration affects the elongation substantially. When the PVA content is too low, no stretching is observed, resulting in spherical iron oxide clusters. Reducing the PVA concentration, the stretching is reduced (Figure S2c) and below 7 wt.% hardly any stretching of the clusters was observed anymore (Figure S2a, b). >10 wt.% PVA concentrations can be used to obtain stretched clusters. However, the viscosity significant increases and a homogeneous mixing of the iron oxide/octane emulsion with the PVA solution becomes difficult. Hence, a PVA concentration of ~10 wt.% is well suited to make ESIONCs with high aspect ratio. The high dependency of the stretching of iron oxide clusters with PVA concentration can be explained by the strong viscosity increase of aqueous solutions with increasing PVA concentration (Figure S3). With an increasing viscosity of the continuous phase, the emulsion

droplets tend to accompany the elongation of the fiber instead of maintaining their spherical shape.

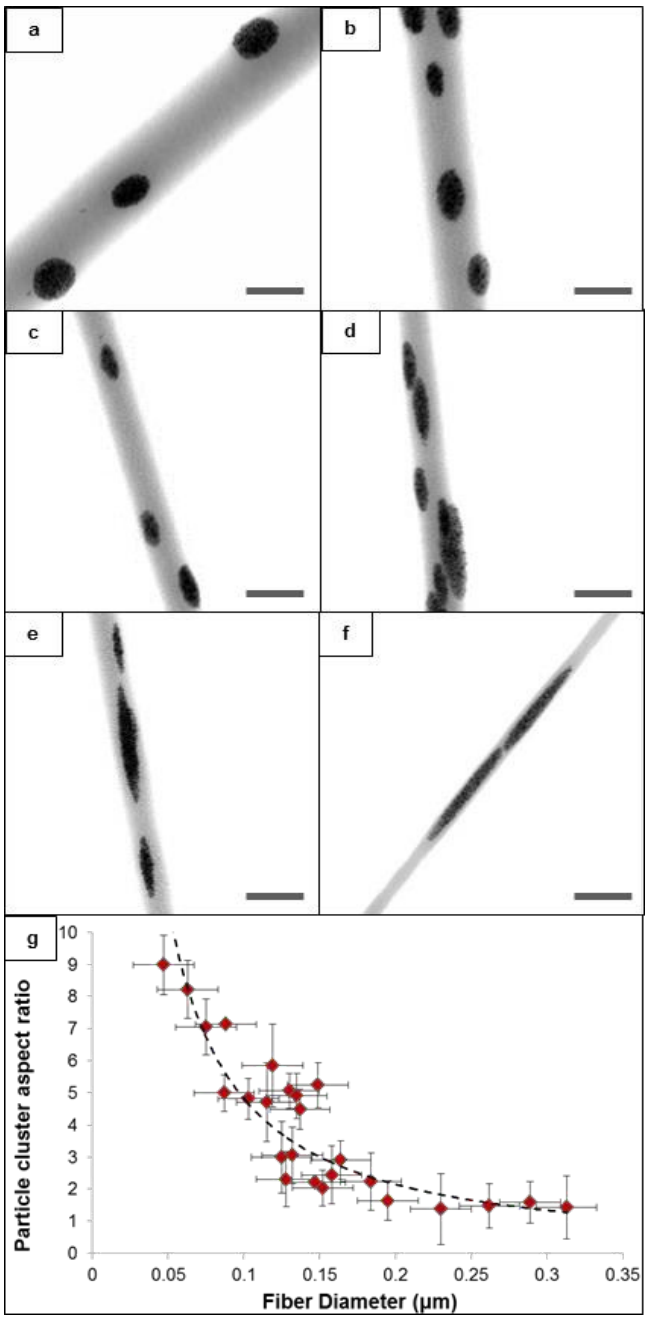

Fig. 3 STEM images of ESIONCs incorporated in electrospun PVA fibers obtained from a 10 wt.% PVA emulsion. With decreasing diameter of the fibers, the aspect ratio of the ESIONCs increases considerably (from a-f). The elongation of the iron oxide clusters occurs mainly independent of the size of the cluster yielding in similar aspect ratio of differently sized particles within the same fiber (d, e). Scale bar: 200 nm. g) Relationship between the aspect ratio of the ESIONCs and the fiber diameter. With a decreasing fiber diameter, the aspect ratio of the ESIONCs increases considerably.

Since the ESIONCs are embedded in a fiber mesh of PVA, the fibers can easily be dissolved in water (see experimental section) and the ESIONCs acquired as an aqueous dispersion (Figure 4a-c). The dispersion shows no significant change in size and polydispersity in a pH range between 3 and 10 as measured by DLS. The mechanical stability of the ESIONCs was tested by putting the ESIONC dispersion in an ultrasonication bath for 1 min. After such treatment one can observe a slight deformation and degradation of the ESIONCs *via* STEM imaging (Figure S5), revealing a vulnerability of the ESIONCs towards ultrasonic treatment. The ESIONCs contain 67 wt.% of iron oxide as determined via thermogravimetric analysis (TGA). The crystal structure was determined from an X-ray diffraction (XRD) pattern and found to be consistent with the structure of magnetite (Figure 4f). The magnetic properties of the ESIONCs were analyzed *via* a Superconducting Quantum Interference Device (SQUID) magnetometer. The measurements reveal a high saturation magnetization value of the ESIONCs (~47 emu·g^{-1} for the clusters themselves and ~70 emu·g^{-1} for the iron oxide part), which is similar to the one of the single oleate-capped iron oxide nanoparticles (Figure S6) and a blocking temperature of around 150 K (Figure 4d, e). Hence, the clusters are the first example of ellipsoid-shaped iron oxide nanoclusters with a high saturation magnetization.

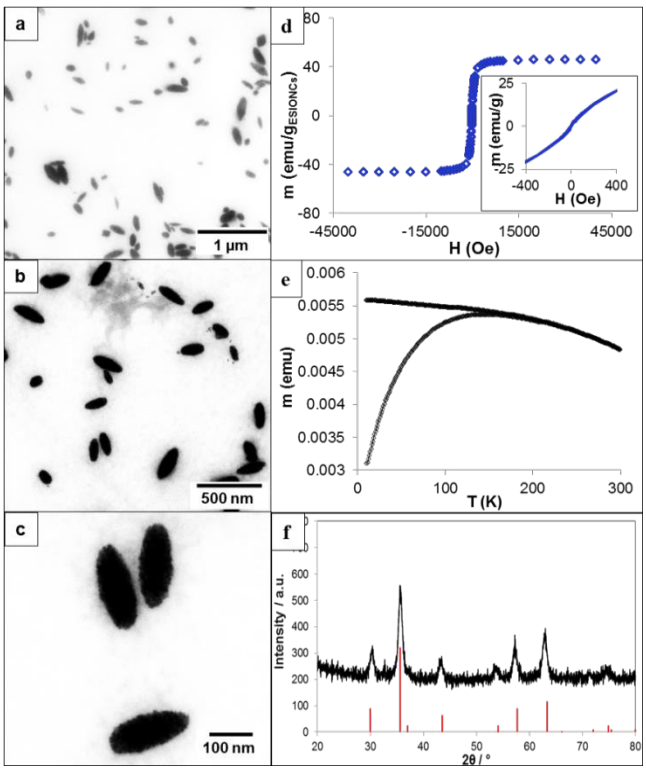

Fig. 4 STEM images of ESIONCs at different magnifications (a-c). The ESIONCs were obtained after dissolving the PVA nanofibers and redispersion of the ESIONCs in water. d) SQUID magnetization curve of ESIONCs at 300 K (with an inset showing no visible hysteresis). e) Temperature dependent magnetization of ESIONCs. f) XRD-pattern of the iron oxide nanoparticles (red peaks correspond to magnetite).

In summary, we have demonstrated for the first time the accumulation of single superparamagnetic iron oxide

nanoparticles into ellipsoid-shape nanoclusters with superparamagnetic properties and a high saturation magnetization. The elongated clusters of iron oxides are generated *via* emulsion electrospinning following an elongation-solvent evaporation mechanism. A strong correlation between the aspect ratio of the obtained ESIONCs and the fiber diameter was found. After elongation, the elongated clusters are embedded in a PVA matrix, which can easily be dissolved with water to yield an aqueous dispersion of the ESIONCs suitable for biomedical applications.

The authors thank Dr. Songhak Yoon for XRD measurements, Manel Beldi for rheology measurements and Lea Bommer for TGA analysis.

Notes and references

[a] Empa, Swiss Federal Laboratories for Materials Science and Technology, Laboratory for Protection and Physiology, Lerchenfeldstrasse 5, CH-9014 St. Gallen, Switzerland.
[b] Institute of Physics, University of Mainz, Staudingerweg 7, 55128 Mainz, Germany.

Electronic Supplementary Information (ESI) available:

1. Neuberger, T.; Schöpf, B.; Hofmann, H.; Hofmann, M.; von Rechenberg, B., *J. Magn. Magn. Mater.* 2005, 293, 483-496.
2. Amstad, E.; Zurcher, S.; Mashaghi, A.; Wong, J. Y.; Textor, M.; Reimhult, E., *Small* 2009, 5, 1334-1342.
3. Hu, F.; MacRenaris, K. W.; A. Waters, E.; Schultz-Sikma, E. A.; Eckermann, A. L.; Meade, T. J., *Chem. Commun*. 2010, 46, 73-75.
4. Jordan, A.; Scholz, R.; Wust, P.; Fahling, H.; Felix, R., *J. Magn. Magn. Mater*. 1999, 201, 413-419.
5. Bannwarth, M. B.; Ebert, S.; Lauck, M.; Ziener, U.; Tomcin, S.; Jakob, G.; Münnemann, K.; Mailänder, V.; Musyanovych, A.; Landfester, K., *Macromolecular Bioscience* 2014, 14, 1205-1214.
6. Teja, A. S.; Koh, P. Y., *Prog. Cryst. Growth Charact. Mater*. 2009, 55, 22-45.
7. Berret, J.-F.; Schonbeck, N.; Gazeau, F.; El Kharrat, D.; Sandre, O.; Vacher, A.; Airiau, M., *J. Am. Chem. Soc.* 2006, 128, 1755-1761.
8. Larsen, B. A.; Haag, M. A.; Serkova, N. J.; Shroyer, K. R.; Stoldt, C. R., *Nanotechnology* 2008, 19.
9. Roch, A.; Gossuin, Y.; Muller, R. N.; Gillis, P., *J. Magn. Magn. Mater*. 2005, 293, 532-539.
10. Ge, J.; Hu, Y.; Biasini, M.; Beyermann, W. P.; Yin, Y., *Angew. Chem. Int. Ed.* 2007, 46, 4342-4345.
11. Leslie-Pelecky, D. L.; Rieke, R. D., *Chem. Mater*. 1996, 8, 1770-1783.
12. Yuan, J. Y.; Xu, Y. Y.; Muller, A. H. E., *Chem. Soc. Rev*. 2011, 40, 640-655.
13. Florez, L.; Herrmann, C.; Cramer, J. M.; Hauser, C. P.; Koynov, K.; Landfester, K.; Crespy, D.; Mailänder, V., *Small* 2012, 8, 2222-2230.
14. Krug, H. F.; Wick, P., *Angew. Chem. Int. Ed*. 2011, 50, 1260-1278.
15. Yunker, P. J.; Still, T.; Lohr, M. A.; Yodh, A. G., *Nature* 2011, 476, 308-311.
16. Bannwarth, M. B.; Kazer, S. W.; Ulrich, S.; Glasser, G.; Crespy, D.; Landfester, K., *Angew. Chem. Int. Ed.* 2013, 52, 10107-10111.
17. Bannwarth, M.; Crespy, D., *Chemistry – An Asian Journal* 2014, 9, 2030-2035.
18. Bannwarth, M. B.; Weidner, T.; Eidmann, E.; Landfester, K.; Crespy, D., *Chem. Mater*. 2014, 26, 1300-1302.
19. Rebolledo, A. F.; Bomatí-Miguel, O.; Marco, J. F.; Tartaj, P., *Adv. Mater*. 2008, 20, 1760-1765.
20. Rebolledo, A. F.; Laurent, S.; Calero, M.; Villanueva, A.; Knobel, M.; Marco, J. F.; Tartaj, P., *ACS Nano* 2010, 4, 2095-2103.
21. Li, L.; Qin, D.; Yang, X.; Liu, G., *Polymer Chemistry* 2010, 1, 289-295.
22. Rebodos, R. L.; Vikesland, P. J., *Langmuir* 2010, 26, 16745-16753.
23. Sanchez-Ferrer, A.; Reufer, M.; Mezzenga, R.; Schurtenberger, P.; Dietsch, H., *Nanotechnology* 2010, 21.
24. Herrmann, C.; Turshatov, A.; Crespy, D., *ACS Macro Letters* 2012, 1, 907-909.
25. Han, T.; Yarin, A. L.; Reneker, D. H., *Polymer* 2008, 49, 1651-1658.
26. Sy, J. C.; Klemm, A. S.; Shastri, V. P., *Adv. Mater*. 2009, 21, 1814-1819.
27. Hofmann, D.; Tenzer, S.; Bannwarth, M. B.; Messerschmidt, C.; Glaser, S.-F.; Schild, H.; Landfester, K.; Mailänder, V., *ACS Nano* 2014, 8, 10077-10088.
28. Camerlo, A.; Bühlmann-Popa, A. M.; Vebert-Nardin, C.; Rossi, R.; Fortunato, G., *Journal of Materials Science* 2014, 49, 8154-8162.
29. Hardick, O.; Stevens, B.; Bracewell, D. G., *Journal of Materials Science* 2011, 46, 3890-3898.
30. Pelipenko, J.; Kristl, J.; Janković, B.; Baumgartner, S.; Kocbek, P., *Int. J. Pharm*. 2013, 456, 125-134.

